Asymptotic densities of planar Lévy walks: A nonisotropic case

Yu. S. Bystrik
Institute of Applied Physics, National Academy of Sciences of Ukraine, Petropavlivska Street 58, 40000 Sumy, Ukraine

S. Denisov
Department of Computer Science, Oslo Metropolitan University, N-0130 Oslo, Norway
and NordSTAR–Nordic Center for Sustainable
and Trustworthy AI Research, Pilestredet 52, Oslo N-0166, Norway

(Received 11 July 2021; accepted 6 December 2021; published 22 December 2021)

Lévy walks are a particular type of continuous-time random walks which results in a super-diffusive spreading of an initially localized packet. The original one-dimensional model has a simple schematization that is based on starting a new unidirectional motion event either in the positive or in the negative direction. We consider two-dimensional generalization of Lévy walks in the form of the so-called XY model. It describes a particle moving with a constant velocity along one of the four basic directions and randomly switching between them when starting a new motion event. We address the ballistic regime and derive solutions for the asymptotic density profiles. The solutions have a form of first-order integrals which can be evaluated numerically. For specific values of parameters we derive an exact expression. The analytic results are in agreement with the results of finite-time numerical samplings.

DOI: 10.1103/PhysRevE.104.064131

I. INTRODUCTION

The idea of Lévy walks (LWs) [1,2] can be sketched as follows: A particle moves, straightforwardly and with the constant velocity v_0, for some time τ_i, then stops, changes, instantaneously and randomly, the direction of its motion, and starts to move along the newly chosen direction. The particle is launched from the origin at the initial instant of time and the process is iterated until the time reaches the set threshold t, $\sum_{i=1}^{N} \tau_i + \bar{\tau}_{N+1} = t$, $0 < \bar{\tau}_{N+1} < \tau_{N+1}$ (that is, the last motion event is stopped once the time threshold is reached). The duration of a motion event is drawn from a probability density function (pdf) with a slowly decaying power-law tail, $\psi(\tau) \propto \tau^{-1-\gamma}$, $0 < \gamma < 2$. During the past two decades, this simple—at first glance—model has found applications in different fields, ranging from physics and chemistry to biology and sociology, as an instrument to describe and understand complex transport phenomena [3].

Most of the existing theoretical results were derived for one-dimensional LW models [3]. Although the 1D setup allows for a lot of flexibility in tailoring of a particular experiment-relevant model, the geometry of the resulting process is simple: the particle moves either to the right or to the left at any instant of time. Generalization of this scheme to 2D is not straightforward and several models have been proposed [2,4], with two of them being most intuitive.

In the *uniform model* [4], the direction of the next flight is determined by choosing, randomly and uniformly, a point on a unit circle (on the surface of the unit sphere $\mathcal{S}^d$ in the d-dimensional case [2,5–7]). The resulting process is spatially isotropic and this allows to reduce the set of spatial variables to a single one, $r = |\mathbf{r}|$.

In the XY model [4,8], the motion of the particle is restricted to four basic Cartesian directions; see Fig. 1. When initiating a new motion event, one has to roll a four-sided die [9], draw duration τ_i, and then set the particle into a ballistic motion along the corresponding direction. The resulting process is essentially nonisotropic and that is imprinted in the shape of pdf $P(\mathbf{r}, t)$ specifying the probability of finding the particle at a vicinity of point $\mathbf{r}$ at time t [4,7]. The XY model is not just an abstract mathematical construction. For example, it reproduces Hamiltonian kinetics in egg-crate potentials [8] and in infinite horizon billiards [10]. Depending on the symmetry of a potential or size of the scatterers in a billiard, the motion can be restricted to four, eight, or larger even number of basic directions [11]. The XY model can be generalized to reproduce kinetics of these systems [12].

In the ballistic regime, $0 < \gamma < 1$, mean flight time $\langle \tau \rangle = \int_0^\infty \tau \psi(\tau)\, d\tau$ diverges and the mean-squared displacement (MSD) of the corresponding LW processes exhibit universal ballistic scaling, $\langle r^2(t) \rangle = \int_0^t r^2 P(\mathbf{r}, t)\, d\tau \propto t^2$. A method to compute asymptotic pdf's for one-dimensional ballistic Lévy walks was presented in Ref. [13]. Consequently, asymptotic pdf's of the uniform model were evaluated in Refs. [5,6].

Here we advance further along this line and address ballistic regime of the XY model. Evidently, the corresponding spatially nonisotropic spreading is more complex than the one generated by the uniform model. Remarkably, as we demonstrate, even in this case it is possible to compute the asymptotic densities and derive analytical expressions.

II. MODEL AND BASIC EQUATIONS

Following the basic idea of LWs [2,3], we consider a particle which moves with constant velocity v_0 and performs instantaneous reorientations at random instants of time. The time between two consequent reorientation events is a random variable distributed according to pdf

$$\psi(\tau) = \frac{1}{\tau_0}\frac{\gamma}{(1+\tau/\tau_0)^{1+\gamma}}, \quad 0 < \gamma < 1, \tag{1}$$

where $\tau_0 > 0$. The reorientation process is determined by pdf $h(\mathbf{v})$ which specifies the direction of vector $\mathbf{v}$, $|\mathbf{v}| = v_0$.

The particle starts from the origin at the initial instant of time. The probability to have the particle moving without reorientation up to time t is $\Psi(t) = \int_t^\infty d\tau\psi(\tau)$. Pdf $P(\mathbf{r}, t)$, after being transformed into the Fourier-Laplace domain, obeys the equation

$$P(\mathbf{k}, s) = \frac{\int d\mathbf{v}\,\Psi(s + i\mathbf{k}\cdot\mathbf{v})h(\mathbf{v})}{1 - \int d\mathbf{v}\,\psi(s + i\mathbf{k}\cdot\mathbf{v})h(\mathbf{v})}, \tag{2}$$

where $\mathbf{k} = \{k_x, k_y\}$ and s are coordinates in the two-dimensional Fourier and one-dimensional Laplace spaces, respectively.

In the case of the XY model, we have reorientation pdf $h(\mathbf{v}) = [\delta(|v_x| - v_0)\delta(v_y) + \delta(v_x)\delta(|v_y| - v_0)]/4$. The ballistic front has the form of a square defined by the equation $|x| + |y| = v_0 t$; see Fig. 1. In this case Eq. (2) can be transformed into

$$P(\mathbf{k}, s) = \frac{\frac{1}{4}[\Psi(s + ik_x v_0) + \Psi(s - ik_x v_0) + \Psi(s + ik_y v_0) + \Psi(s - ik_y v_0)]}{1 - \frac{1}{4}[\psi(s + ik_x v_0)] + \psi(s - ik_x v_0) - \psi(s + ik_y v_0) - \psi(s - ik_y v_0)]}.$$

By multiplying both the numerator and the denominator by 4 and grouping the terms in the denominator, we get

$$P(\mathbf{k}, s) = \frac{\sum_{\kappa\in\mathcal{K}}\Psi(s + i\kappa v_0)}{\sum_{\kappa\in\mathcal{K}}[1 - \psi(s + i\kappa v_0)]}, \tag{3}$$

where $\mathcal{K} = \{\pm k_x, \pm k_y\}$. The structure of the equation highlights the fact that $P(\mathbf{r}, t)$ is an even (symmetric) function with respect to the space coordinates and is also invariant under permutation $x \leftrightarrow y$. Henceforth, we assume that $v_0 = 1$ and consistently renormalized time which now is measure in units of space. It would be enough to replace $t \mapsto v_0 t$ in the final expressions to obtain the answer for arbitrary v_0.

In the long-time limit, the waiting-time distribution Eq. (1) can be approximated in the Laplace domain as

$$\psi(s) \simeq 1 - \tau_0^\gamma \Gamma(1-\gamma)s^\gamma + O(s). \tag{4}$$

In the limit $\mathbf{k}, s \to 0$ (which corresponds to both $\mathbf{r}$ and t are going to infinity), we obtain from Eqs. (3) and (4) the following expression:

$$P_{XY}(\mathbf{k}, s) = \frac{\sum_{\kappa\in\mathcal{K}}(s + i\kappa)^{\gamma-1}}{\sum_{\kappa\in\mathcal{K}}(s + i\kappa)^\gamma}. \tag{5}$$

Note that, in this limit, s and components of $\mathbf{k}$ are comparable, i.e., they approach zero with comparable speeds. This implies that, in the original domain, the components of vector $\mathbf{r}/(v_0 t)$ are of the order $O(1)$.

It is noteworthy that, by using the notion of fractional material derivatives [14–16], a deterministic equation governing the evolution of the pdf in the original space, can be derived.

III. DERIVATION OF ASYMPTOTIC PDF $\mathcal{P}(\bar{x}, \bar{y})$

We start with recasting Eq. (5) into

$$P_{XY}(\mathbf{k}, s) = Q(k_x, k_y, s) + Q(k_y, k_x, s), \tag{6}$$

where

$$Q(k_x, k_y, s) = \frac{(s + ik_x)^{\gamma-1} + (s - ik_x)^{\gamma-1}}{\sum_{\kappa\in\mathcal{K}}(s + i\kappa)^\gamma}. \tag{7}$$

It is enough therefore to find the inverse of function $Q(k_x, k_y, s)$ [the inverse of $Q(k_y, k_x, s)$ could be obtained by permuting $x \leftrightarrow y$].

We introduce the following two functions:

$$g_1\left(\frac{ik_x}{s}, u\right) = \left[\left(1 + \frac{ik_x}{s}\right)^{\gamma-1} + \left(1 - \frac{ik_x}{s}\right)^{\gamma-1}\right]\exp\left\{-u\left[\left(1 + \frac{ik_x}{s}\right)^\gamma + \left(1 - \frac{ik_x}{s}\right)^\gamma\right]\right\}, \tag{8}$$

$$g_2\left(\frac{ik_y}{s}, u\right) = \exp\left\{-u\left[\left(1 + \frac{ik_y}{s}\right)^\gamma + \left(1 - \frac{ik_y}{s}\right)^\gamma\right]\right\}. \tag{9}$$

By implementing identity

$$1/\varrho = \int_0^\infty du\, e^{-u\varrho} \ (\mathrm{Re}\,\varrho > 0), \tag{10}$$

we can recast Eq. (7) as

$$Q(k_x, k_y, s) = \frac{1}{s}\int_0^\infty du\, g_1\left(\frac{ik_x}{s}, u\right)g_2\left(\frac{ik_y}{s}, u\right). \tag{11}$$

By using properties of the Laplace transform for a derivative and a convolution (which we denote with $\circ$), from Eq. (11) we obtain

$$Q(x, y, t) = \frac{\partial}{\partial t}\int_0^\infty du\, G_1(x, t, u) \circ G_2(y, t, u), \tag{12}$$

where

$$G_1(x, t, u) = \mathcal{F}_x^{-1}\mathcal{L}^{-1}\left\{\frac{1}{s}g_1\left(\frac{ik_x}{s}, u\right)\right\}, \tag{13}$$

$$G_2(y, t, u) = \mathcal{F}_y^{-1}\mathcal{L}^{-1}\left\{\frac{1}{s}g_2\left(\frac{ik_y}{s}, u\right)\right\}. \tag{14}$$

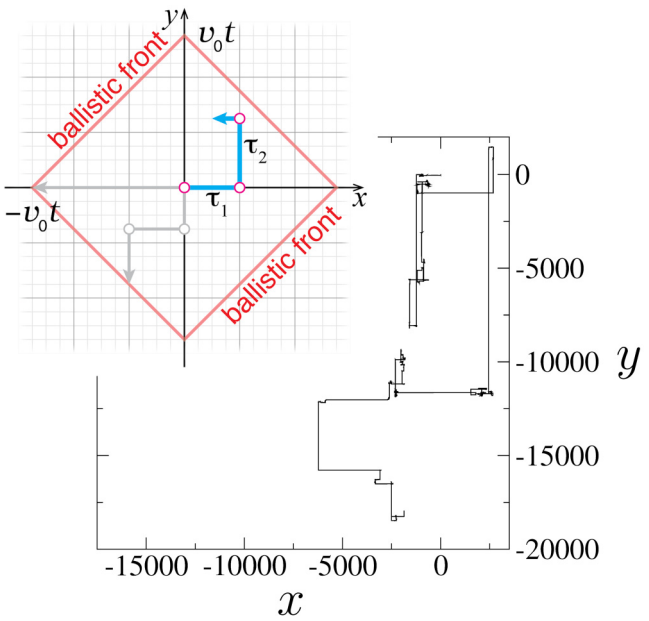

FIG. 1. *XY* model of planar Lévy walks. A particle is allowed to move, with a speed v_0, only along one Cartesian axis at a time, which is chosen randomly at the reorientation points ○. The ballistic front is determined by the square $|x| + |y| = v_0 t$. Geometry of the process imparts the shape of the corresponding trajectory which exhibits a distinctive rectangular weblike pattern with long ballistic relocations along the two axes. The parameters here are $\gamma = 1/2$, $v_0 = 1$ and $\tau_0 = 1$.

Thus, we obtained the expression for $Q(x, y, t)$ which demands not a three-step inverse transform, $\mathcal{F}_x^{-1}\mathcal{F}_y^{-1}\mathcal{L}^{-1}$, but a pair of two-step inverse transforms, $\mathcal{F}_x^{-1}\mathcal{L}^{-1}$ and $\mathcal{F}_y^{-1}\mathcal{L}^{-1}$, of functions $\frac{1}{s}g_1(\frac{ik_x}{s})$ and $\frac{1}{s}g_2(\frac{ik_y}{s})$, respectively. To find the inverses, we follow a procedure similar to that given in Ref. [17] (see Appendix A) and obtain

$$G_1(x,t,u) = -\frac{1}{2\pi i x}\lim_{\epsilon\to 0^+}\left[g_1\left(-\frac{1}{x/t+i\epsilon},u\right) - g_1^*\left(-\frac{1}{x/t+i\epsilon},u\right)\right] \tag{15}$$

and

$$G_2(y,t,u) = -\frac{1}{2\pi i y}\lim_{\epsilon\to 0^+}\left[g_2\left(-\frac{1}{y/t+i\epsilon},u\right) - g_2^*\left(-\frac{1}{y/t+i\epsilon},u\right)\right]. \tag{16}$$

For the principal values of functions $(1 \pm \zeta)^\gamma$ the following holds:

$$\lim_{\epsilon\to 0^+}(1+\zeta)^\gamma\big|_{\zeta=-1/(\xi\pm i\epsilon)} = |1-1/\xi|^\gamma e^{\pm i\pi\gamma\mathbb{1}_{(0,1)}(\xi)},$$

$$\lim_{\epsilon\to 0^+}(1-\zeta)^\gamma\big|_{\zeta=-1/(\xi\pm i\epsilon)} = |1+1/\xi|^\gamma e^{\mp i\pi\gamma\mathbb{1}_{(-1,0)}(\xi)},$$

where we use the indicator function

$$\mathbb{1}_{\mathcal{A}}(\xi) = \begin{cases} 1, & \xi \in \mathcal{A}, \\ 0, & \xi \notin \mathcal{A}. \end{cases} \tag{17}$$

Taking into account that both functions, $G_1(x,t,u)$ and $G_2(y,t,u)$, are even (symmetric) with respect to x and y [this trivially follows from the fact that functions Eqs. (8) and (9) are even with respect to k_x and k_y], we can rewrite Eqs. (13) and (14) in the following form:

$$G_1(x,t,u) = -\frac{\mathbb{1}_{(0,t)}(|x|)}{2\pi i\,|x|}\left[h_{\gamma-1}\left(\frac{|x|}{t}\right)e^{-uh_\gamma(\frac{|x|}{t})} - h^*_{\gamma-1}\left(\frac{|x|}{t}\right)e^{-uh^*_\gamma(\frac{|x|}{t})}\right], \tag{18}$$

$$G_2(y,t,u) = -\frac{\mathbb{1}_{(0,t)}(|y|)}{2\pi i\,|y|}\left[e^{-uh_\gamma(\frac{|y|}{t})} - e^{-uh^*_\gamma(\frac{|y|}{t})}\right], \tag{19}$$

where

$$h_\gamma(\xi) = |1-1/\xi|^\gamma e^{i\pi\gamma} + |1+1/\xi|^\gamma. \tag{20}$$

Substituting Eqs. (18) and (19) into Eq. (12), after some derivation, we obtain

$$Q(x,y,t) = \frac{\mathbb{1}_{(0,t)}(|x|+|y|)}{2\pi^2|x||y|}\mathrm{Re}\,\frac{\partial}{\partial t}\int_{|y|}^{t-|x|} d\tau\, h_{\gamma-1}\left(\frac{|x|}{t-\tau}\right) \times\left[\frac{1}{h_\gamma(\frac{|x|}{t-\tau}) + h^*_\gamma(\frac{|y|}{\tau})} - \frac{1}{h_\gamma(\frac{|x|}{t-\tau}) + h_\gamma(\frac{|y|}{\tau})}\right]. \tag{21}$$

Finally, by substituting $\tau = (t-|x|-|y|)\eta + |y|$ and introducing notations

$$x_t = \frac{2|x|}{t-|x|-|y|}, \quad y_t = \frac{2|y|}{t-|x|-|y|}, \tag{22}$$

pdf $P_{XY}(x,y,t)$ can be represented as

$$P_{XY}(x,y,t) = Q(x,y,t) + Q(y,x,t), \tag{23}$$

where

$$Q(x,y,t) = \frac{1}{2\pi^2|y|}\mathrm{Re}\frac{\partial}{\partial t}R(x_t,y_t) \tag{24}$$

and

$$R(x_t,y_t) = x_t^{-\gamma}\int_0^1 d\eta[(1-\eta)^{\gamma-1}e^{i\pi(\gamma-1)} + (1-\eta+x_t)^{\gamma-1}]\left\{\frac{1}{x_t^{-\gamma}[(1-\eta)^\gamma e^{i\pi\gamma} + (1-\eta+x_t)^\gamma] + y_t^{-\gamma}[\eta^\gamma e^{-i\pi\gamma} + (\eta+y_t)^\gamma]} - \frac{1}{x_t^{-\gamma}[(1-\eta)^\gamma e^{i\pi\gamma} + (1-\eta+x_t)^\gamma] + y_t^{-\gamma}[\eta^\gamma e^{i\pi\gamma} + (\eta+y_t)^\gamma]}\right\} \tag{25}$$

if $|x| + |y| < t$ and $P_{XY}(x,y,t) = 0$ if otherwise [henceforth, we assume that $Q(x,y,t)$ and all related functions are multiplied with the indicator function, Eq. (17)]. Again, expressions for $Q(y,x,t)$ and $R(y_t,x_t)$ can be obtained from Eqs. (24) and (25) by permuting $x \leftrightarrow y$.

It will be easier to compute $P_{XY}(x,y,t)$ if we take derivative with respect to time in Eq. (24) and in the corresponding expression for $Q(y,x,t)$. As the result we obtain

$$P_{XY}(x,y,t) = Q_1(x,y,t) + Q_2(x,y,t) + Q_1(y,x,t) + Q_2(y,x,t), \tag{26}$$

where

$$Q_1(x,y,t) = \frac{(1-\gamma)x_t^{1-\gamma}y_t}{4\pi^2|y|^2}\int_0^1 d\eta(1-\eta+x_t)^{\gamma-2}\mathrm{Re}\Bigg\{\frac{1}{x_t^{-\gamma}[(1-\eta)^\gamma e^{i\pi\gamma}+(1-\eta+x_t)^\gamma]+y_t^{-\gamma}[\eta^\gamma e^{-i\pi\gamma}+(\eta+y_t)^\gamma]} - \frac{1}{x_t^{-\gamma}[(1-\eta)^\gamma e^{i\pi\gamma}+(1-\eta+x_t)^\gamma]+y_t^{-\gamma}[\eta^\gamma e^{i\pi\gamma}+(\eta+y_t)^\gamma]}\Bigg\}, \tag{27}$$

$$Q_2(x,y,t) = \frac{\gamma x_t^{-\gamma}y_t}{4\pi^2|y|^2}\int_0^1 d\eta\big[x_t^{1-\gamma}(1-\eta+x_t)^{\gamma-1}+y_t^{1-\gamma}(\eta+y_t)^{\gamma-1}\big]\mathrm{Re}\big[(1-\eta)^{\gamma-1}e^{i\pi(\gamma-1)}+(1-\eta+x_t)^{\gamma-1}\big] \times\Bigg\{\frac{1}{\big\{x_t^{-\gamma}[(1-\eta)^\gamma e^{i\pi\gamma}+(1-\eta+x_t)^\gamma]+y_t^{-\gamma}[\eta^\gamma e^{-i\pi\gamma}+(\eta+y_t)^\gamma]\big\}^2} - \frac{1}{\big\{x_t^{-\gamma}[(1-\eta)^\gamma e^{i\pi\gamma}+(1-\eta+x_t)^\gamma]+y_t^{-\gamma}[\eta^\gamma e^{i\pi\gamma}+(\eta+y_t)^\gamma]\big\}^2}\Bigg\}. \tag{28}$$

By introducing coordinates

$$\bar{x} = \frac{1}{t}\int_0^t v(t')dt' = \frac{x}{t}, \quad \bar{y} = \frac{1}{t}\int_0^t v(t')dt' = \frac{y}{t}, \tag{29}$$

for which the pdf has the form

$$\mathcal{P}(\bar{x},\bar{y}) = t^2 P_{XY}(t\bar{x},t\bar{y},t), \tag{30}$$

we can obtain an expression that does not depend on t in the explicit way. We will not write it here; it can be obtained straightforwardly from Eq. (26) by replacing $x\to\bar{x}$, $y\to\bar{y}$ and $t\to 1$.

IV. ALTERNATIVE REPRESENTATION OF $\mathcal{P}(\bar{x},\bar{y})$

Here we derive an alternative expression for $P_{XY}(x,y,t)$ which will be used to derive exact analytical expression for $\gamma=\frac{1}{2}$ in Sec. VI.

First, we recast Eq. (5) as

$$P_{XY}(\mathbf{k},s) = H(k_x,k_y,s) + H(-k_x,k_y,s) + H(k_y,k_x,s) + H(-k_y,k_x,s), \tag{31}$$

where

$$H(k_x,k_y,s) = \frac{(s+ik_x)^{\gamma-1}}{\sum_{\kappa\in\mathcal{K}}(s+i\kappa)^\gamma}. \tag{32}$$

We use Eq. (10), together with the definition of the Laplace transform of a convolution, to obtain

$$H(x,y,t) = \int_0^\infty du\, H_1(x,t,u)\circ H_2(y,t,u), \tag{33}$$

where

$$H_1(x,t,u) = \mathcal{F}_x^{-1}\mathcal{L}^{-1}\big\{(s+ik_x)^{\gamma-1}e^{-u(s+ik_x)^\gamma}e^{-u(s-ik_x)^\gamma}\big\}, \tag{34}$$

$$H_2(y,t,u) = \mathcal{F}_y^{-1}\mathcal{L}^{-1}\big\{e^{-u(s+ik_y)^\gamma}e^{-u(s-ik_y)^\gamma}\big\}. \tag{35}$$

Next we use the property of the Fourier transform of a convolution (which we denote with $\bullet$) to rewrite Eqs. (34) and (35) as

$$H_1(x,t,u) = \mathcal{F}_x^{-1}\mathcal{L}^{-1}\big\{(s+ik_x)^{\gamma-1}e^{-u(s+ik_x)^\gamma}\big\} \times\circ\bullet_x \mathcal{F}_x^{-1}\mathcal{L}^{-1}\big\{e^{-u(s-ik_x)^\gamma}\big\}, \tag{36}$$

$$H_2(y,t,u) = \mathcal{F}_y^{-1}\mathcal{L}^{-1}\big\{e^{-u(s+ik_y)^\gamma}\big\} \times\circ\bullet_y \mathcal{F}_y^{-1}\mathcal{L}^{-1}\big\{e^{-u(s-ik_y)^\gamma}\big\}. \tag{37}$$

It is now clear that we are dealing with one-sided γ-stable Lévy distribution $\ell_\gamma(t)=\mathcal{L}^{-1}\{e^{-s^\gamma}\}$ [18]. It is easy to see that for $u>0$ we have

$$\mathcal{L}^{-1}\big\{e^{-us^\gamma}\big\} = u^{-1/\gamma}\ell_\gamma(u^{-1/\gamma}t),$$

$$\mathcal{L}^{-1}\big\{s^{\gamma-1}e^{-us^\gamma}\big\} = \frac{t}{\gamma u}u^{-1/\gamma}\,\ell_\gamma(u^{-1/\gamma}t).$$

Using these expressions together with the property of a shifted inverse Laplace transform, $\mathcal{L}^{-1}\{f(s+b)\}=e^{-bt}f(t)$, and the fact that $\mathcal{F}_x^{-1}\{e^{-ik_xb}\}=\delta(x+b)$ (the same stands for y), from Eqs. (36) and (37) we obtain

$$H_1(x,t,u) = \mathbb{1}_{(0,t)}(|x|)\frac{u^{-2/\gamma-1}}{2\gamma}\frac{t+x}{2}\ell_\gamma\Big(\frac{t+x}{2u^{1/\gamma}}\Big)\ell_\gamma\Big(\frac{t-x}{2u^{1/\gamma}}\Big) \tag{38}$$

and

$$H_2(y,t,u) = \mathbb{1}_{(0,t)}(|y|)\frac{u^{-2/\gamma}}{2}\ell_\gamma\Big(\frac{t+y}{2u^{1/\gamma}}\Big)\ell_\gamma\Big(\frac{t-y}{2u^{1/\gamma}}\Big). \tag{39}$$

Substituting Eqs. (38) and (39) into Eq. (33), we get

$$H(x,y,t) = \frac{\mathbb{1}_{(0,t)}(|x|+|y|)}{8\gamma}\int_0^\infty du\, u^{-4/\gamma-1} \times\int_{|y|}^{t-|x|} d\tau\,(t-\tau+x) \times\ell_\gamma\Big(\frac{t-\tau+x}{2u^{1/\gamma}}\Big)\ell_\gamma\Big(\frac{t-\tau-x}{2u^{1/\gamma}}\Big) \times\ell_\gamma\Big(\frac{\tau+y}{2u^{-1/\gamma}}\Big)\ell_\gamma\Big(\frac{\tau-y}{2u^{-1/\gamma}}\Big). \tag{40}$$

Finally, by changing variables, $\tau = (t - |x| - |y|)\eta + |y|$ for the internal integral in Eq. (40) and $u = (\frac{t-|x|-|y|}{2})^{\gamma}\vartheta$ for the external one, from $P_{XY}(x,y,t) = H(x,y,t) + H(-x,y,t) + H(y,x,t) + H(-y,x,t)$ [see Eq. (31)] we obtain

$$P_{XY}(x,y,t) = \frac{4t}{\gamma(t-|x|-|y|)^3}\int_0^\infty d\vartheta\,\vartheta^{-4/\gamma-1} \times \int_0^1 d\eta\,\ell_\gamma\left(\frac{1-\eta}{\vartheta^{1/\gamma}}\right)\ell_\gamma\left(\frac{\eta}{\vartheta^{1/\gamma}}\right) \times \ell_\gamma\left(\frac{1-\eta+x_t}{\vartheta^{1/\gamma}}\right)\ell_\gamma\left(\frac{\eta+y_t}{\vartheta^{1/\gamma}}\right) \quad (41)$$

if $|x| + |y| < t$ and $P_{XY}(x,y,t) = 0$ if otherwise.

Equation (66) is less complex than the one obtained in the previous section but it includes a double integral and seems to be less convenient for numerical evaluation. However, as we will show in Sec. VI, this form allows us to derive an exact analytic expression for the case $\gamma = 1/2$. Moreover, from this representation we see that $P_{XY}(x,y,t)$ is indeed a nonnegative function and hence it is a legitimate pdf [while the normalization condition is obviously holds due to the fact that $P_{XY}(\mathbf{k},s)|_{\mathbf{k}=0} = 1/s$].

By changing variables in Eq. (66), $\vartheta^{-1/\gamma} \mapsto \vartheta$, $\bar{x} = x/t$, and $\bar{y} = y/t$, and introducing new variables,

$$x_r = \frac{2|\bar{x}|}{1-|\bar{x}|-|\bar{y}|}, \quad y_r = \frac{2|\bar{y}|}{1-|\bar{x}|-|\bar{y}|}, \quad (42)$$

we obtain the following expression for $\mathcal{P}(\bar{x},\bar{y})$:

$$\mathcal{P}(\bar{x},\bar{y}) = \frac{4}{(1-|\bar{x}|-|\bar{y}|)^3}\int_0^\infty d\vartheta\,\vartheta^3\int_0^1 d\eta\,\ell_\gamma[\vartheta(1-\eta)] \times \ell_\gamma(\vartheta\eta)\ell_\gamma[\vartheta(1-\eta+x_r)]\ell_\gamma[\vartheta(\eta+y_r)], \quad (43)$$

when $|\bar{x}| + |\bar{y}| < 1$ and $\mathcal{P}(\bar{x},\bar{y}) = 0$ otherwise [19].

V. NUMERICAL ANALYSIS

A. Numerical evaluation of $\mathcal{P}(\bar{x},\bar{y})$

Here we show how to compute asymptotic pdf $\mathcal{P}(\bar{x},\bar{y})$. From Eq. (26) we have

$$\mathcal{P}(\bar{x},\bar{y}) = Q_1(\bar{x},\bar{y}) + Q_2(\bar{x},\bar{y}) + Q_1(\bar{y},\bar{x}) + Q_2(\bar{y},\bar{x}), \quad (44)$$

where $Q_{1,2}(\bar{x},\bar{y}) = Q_{1,2}(\bar{x},\bar{y},t=1)$. In Eqs. (27) and (28) we replace variable $\eta \mapsto \frac{1+\eta}{2}$. This allows us to extend the integration interval from $[0,1]$ to $[-1,1]$ and then implement Gauss–Jacobi quadrature [20]. We chose this particular method because it is very convenient to deal numerically with integrals which includes power-law singularities.

We now write

$$Q_1(\bar{x},\bar{y}) = \int_{-1}^1 d\eta\,(1-\eta)^{\gamma-1}q_1(\eta;\bar{x},\bar{y}), \quad (45)$$

$$Q_2(\bar{x},\bar{y}) = \int_{-1}^1 d\eta\,(1-\eta)^{\gamma-1}q_2(\eta;\bar{x},\bar{y}), \quad (46)$$

with functions

$$q_1(\eta;\bar{x},\bar{y}) = \frac{2(1-\gamma)}{\pi^2 x_r^{\gamma-1}y_r(1-|\bar{x}|-|\bar{y}|)^2}(1-\eta)^{1-\gamma}(1-\eta+2x_r)^{\gamma-2} \times \mathrm{Re}\left\{\frac{1}{x_r^{-\gamma}[(1-\eta)^\gamma e^{i\pi\gamma} + (1-\eta+2x_r)^\gamma] + y_r^{-\gamma}[(1+\eta)^\gamma e^{-i\pi\gamma} + (1+\eta+2y_r)^\gamma]} - \frac{1}{x_r^{-\gamma}[(1-\eta)^\gamma e^{i\pi\gamma} + (1-\eta+2x_r)^\gamma] + y_r^{-\gamma}[(1+\eta)^\gamma e^{i\pi\gamma} + (1+\eta+2y_r)^\gamma]}\right\}, \quad (47)$$

$$q_2(\eta;\bar{x},\bar{y}) = \frac{2\gamma}{\pi^2 x_r^\gamma y_r(1-|\bar{x}|-|\bar{y}|)^2}\left[x_r^{1-\gamma}(1-\eta+2x_r)^{\gamma-1} + y_r^{1-\gamma}(1+\eta+2y_r)^{\gamma-1}\right] \times \mathrm{Re}\left[e^{i\pi(\gamma-1)} + (1-\eta)^{1-\gamma}(1-\eta+2x_r)^{\gamma-1}\right] \times \left\{\frac{1}{\left\{x_r^{-\gamma}[(1-\eta)^\gamma e^{i\pi\gamma} + (1-\eta+2x_r)^\gamma] + y_r^{-\gamma}[(1+\eta)^\gamma e^{-i\pi\gamma} + (1+\eta+2y_r)^\gamma]\right\}^2} - \frac{1}{\left\{x_r^{-\gamma}[(1-\eta)^\gamma e^{i\pi\gamma} + (1-\eta+2x_r)^\gamma] + y_r^{-\gamma}[(1+\eta)^\gamma e^{i\pi\gamma} + (1+\eta+2y_r)^\gamma]\right\}^2}\right\}, \quad (48)$$

which have no singularities with respect to η (for any fixed values of $\bar{x}$ and $\bar{y}$).

Following the Gauss–Jacobi quadrature recipe [20], we obtain

$$Q_1(\bar{x},\bar{y}) \approx \sum_{j=1}^n w_j q_1(\eta_j;\bar{x},\bar{y}), \quad (49)$$

$$Q_2(\bar{x},\bar{y}) \approx \sum_{j=1}^n w_j q_2(\eta_j;\bar{x},\bar{y}), \quad (50)$$

where weights are

$$w_j = -\frac{(2n+a+b+2)\Gamma(n+a+1)}{(n+a+b+1)^2\Gamma(n+a+b+1)} \times \frac{\Gamma(n+b+1)2^{a+b+1}}{\Gamma(n+2)J_{n-1}^{(a+1,b+1)}(\eta_j)J_{n+1}^{(a,b)}(\eta_j)} \quad (51)$$

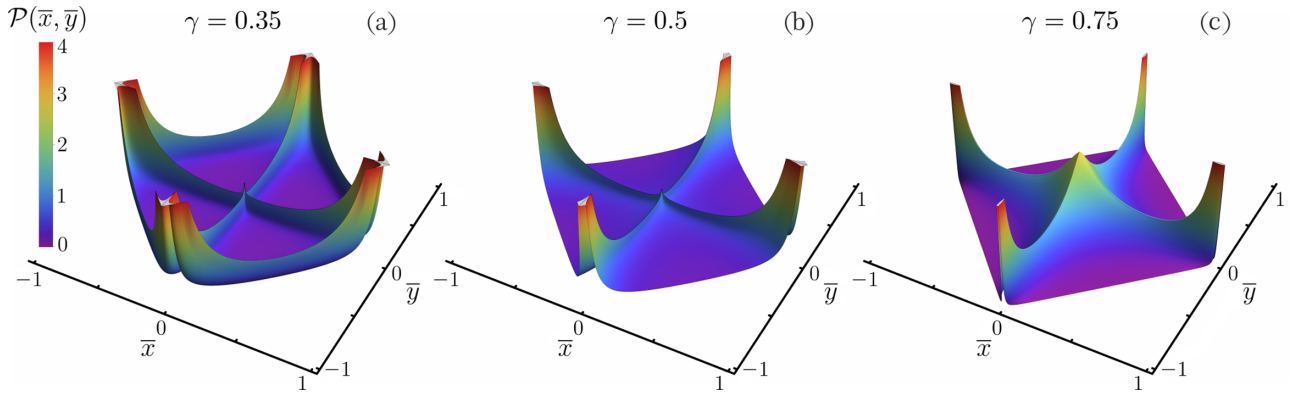

FIG. 2. Asymptotic probability density functions $\mathcal{P}(\bar{x},\bar{y})$ for different values of γ. The functions are obtained by using Eq. (44). Note that in cases (a) and (b) $\mathcal{P}(\bar{x},\bar{y})$ is singular along lines $\bar{x}=0$ and $\bar{y}=0$, while minimal absolute values of $\bar{x}$ and $\bar{y}$ used to plot the functions are 10^{-3}. In the case (a), $\mathcal{P}(\bar{x},\bar{y})$ is also singular along the ballistic front $|x|+|y|=1$ and the outward points used to plot the functions are at distance 10^{-3} from the front.

and η_j are roots of Jacobi polynomials $J_n^{(a,b)}(\eta)$. In our case $a=\gamma-1$ and $b=0$.

In the functions under the integrals in Eqs. (45) and (46), we separate singular multiplier $(1-\eta)^{\gamma-1}$, and then compensate it with $(1-\eta)^{1-\gamma}$ in some places [21]. Figure 2 shows asymptotic pdf computed for three different values of γ. Note that, for $\gamma=0.35$ and 0.5, the corresponding pdf's are singular along lines $\bar{x}=0$ and $\bar{y}=0$ [22]. Additionally, for $\gamma=0.35$, the pdf is also singular along the ballistic front [22]. The numerically calculated pdf's have finite height because the minimal distances of the grid points from the singular lines are 10^{-3}.

B. Comparison with the results of finite-time samplings

Here we discuss a procedure to compare analytical results with numerically sampled finite-time histograms.

We first split the domain where the pdf takes nonzero values, i.e., inside the ballistic square $|\bar{x}|+|\bar{y}|<1$, into a set of bins.

Consider now bin $\mathcal{A}$ of area $S(\mathcal{A})$. Then the average probability density function over bin $\mathcal{A}$ is

$$\mathcal{P}_{\mathcal{A}}=\frac{1}{S(\mathcal{A})}\iint_{\mathcal{A}}\mathcal{P}(\bar{x},\bar{y})d\bar{x}d\bar{y}. \tag{52}$$

The corresponding pdf (which will be estimated through the numerical sampling) is

$$\mathcal{P}^{\rm num}_{\mathcal{A}}=\frac{1}{S(\mathcal{A})}\frac{N_{\mathcal{A}}}{N_{\rm total}}. \tag{53}$$

Here $N_{\mathcal{A}}$ is the number of realizations which ended up, after fixed time t, in bin $\mathcal{A}$, while $N_{\rm total}$ is the total number of realizations. Then, for large enough $N_{\rm total}$, we expect $\mathcal{P}_{\mathcal{A}}\approx\mathcal{P}^{\rm num}_{\mathcal{A}}$.

If function $\mathcal{P}(\bar{x},\bar{y})$ is continuous over $\mathcal{A}$, then, according to the mean value theorem, there is point $(\bar{x}_c,\bar{y}_c)\in\mathcal{A}$ such that $\mathcal{P}_{\mathcal{A}}=\mathcal{P}(\bar{x}_c,\bar{y}_c)$. If, in addition, $\mathcal{A}$ is small (compared to the characteristic scale over which $\mathcal{P}_{\mathcal{A}}$ varies substantially), then, by using Taylor series, we have $\mathcal{P}(\bar{x},\bar{y})\approx\mathcal{P}(\bar{x}_c,\bar{y}_c)$ for all $(\bar{x},\bar{y})\in\mathcal{A}$. Therefore, in a sufficiently small domain $\mathcal{A}$, pdf $\mathcal{P}(\bar{x},\bar{y})$ can be approximated by the average density over the domain such that $\mathcal{P}(\bar{x},\bar{y})|_{(\bar{x},\bar{y})\in\mathcal{A}}\approx\mathcal{P}_{\mathcal{A}}\approx\mathcal{P}^{\rm num}_{\mathcal{A}}$.

We partition the interior of square $|\bar{x}|+|\bar{y}|<1$ into set of bins with a set of lines parallel to the main Cartesian axes and distance ε between two neighboring lines. By doing that, we obtain M^2 bins, $M=2/\varepsilon$.

Bin $\mathcal{A}_{ij}$ is defined as $\bar{x}_i\leqslant\bar{x}\leqslant\bar{x}_{i+1}$ and $\bar{y}_j\leqslant\bar{y}\leqslant\bar{y}_{j+1}$ with $\bar{x}_{i+1}-\bar{x}_i=\bar{y}_{j+1}-\bar{y}_j=\varepsilon$. We have

$$\begin{aligned}\mathcal{P}_{\mathcal{A}_{ij}}&=\frac{1}{S(\mathcal{A}_{ij})}\iint_{\mathcal{A}_{ij}}\mathcal{P}(\bar{x},\bar{y})d\bar{x}d\bar{y}\\&=\frac{1}{\varepsilon^2}\int_{\bar{x}_i}^{\bar{x}_{i+1}}\int_{\bar{y}_j}^{\bar{y}_{j+1}}\mathcal{P}(\bar{x},\bar{y})d\bar{x}d\bar{y}.\end{aligned}$$

By introducing variables $\bar{x}=\frac{\bar{x}_{i+1}-\bar{x}_i}{2}x'+\frac{\bar{x}_{i+1}+\bar{x}_i}{2}$ and $\bar{y}=\frac{\bar{y}_{j+1}-\bar{y}_j}{2}y'+\frac{\bar{y}_{j+1}+\bar{y}_j}{2}$, which maps intervals $[\bar{x}_i,\bar{x}_{i+1}]$ and $[\bar{y}_j,\bar{y}_{j+1}]$ onto the interval $[-1,1]$, we get

$$\begin{aligned}\mathcal{P}_{\mathcal{A}_{ij}}&=\frac{1}{4}\int_{-1}^{1}\int_{-1}^{1}\mathcal{P}\Big[\frac{\varepsilon}{2}(x'+1)+\bar{x}_i,\frac{\varepsilon}{2}(y'+1)+\bar{y}_j\Big]dx'dy'\\&\approx\frac{1}{4}\sum_{m_1=1}^{m}\sum_{m_2=1}^{m}w_{m_1}w_{m_2}\mathcal{P}\Big[\frac{\varepsilon}{2}(x'_{m_1}+1)\\&\quad+\bar{x}_i,\frac{\varepsilon}{2}(y'_{m_2}+1)+\bar{y}_j\Big].\end{aligned} \tag{54}$$

In the second line of Eq. (54) we approximated the integral by using orthogonal Legendre polynomials of order m (they can be obtained as a particular case of Jacobi polynomials by setting $a=b=0$). Therefore, in this case weights w_{m_1,m_2} follow from Eq. (51) with $a=b=0$, while x_{m_1} and y_{m_2} are roots of Legendre polynomial $P_m(\xi)=J_m^{(0,0)}(\xi)$. To find $\mathcal{P}_{\mathcal{A}_{ij}}$, we have to calculate $\mathcal{P}[\frac{\varepsilon}{2}(x'_{m1}+1)+\bar{x}_i,\frac{\varepsilon}{2}(y'_{m2}+1)+\bar{y}_j]$ by using the above described method. For the bins in which $\mathcal{P}(\bar{x},\bar{y})$ has singularities [22], we can use the same scheme, by taking into account the corresponding singularity order in Eq. (54).

We denote the averaged (over the bin) probability density $\mathcal{P}_{\mathcal{A}_{ij}}$ as $\mathcal{P}_{\rm bin}(\bar{x},\bar{y})$, where $(\bar{x},\bar{y})$ are coordinates of the center of bin $\mathcal{A}_{ij}$. Figures 3–6 present probability density functions obtained by averaging pdf $\mathcal{P}(\bar{x},\bar{y})$, Eq. (30), over the bins of a 400×400 grid, together with normalized histograms (by

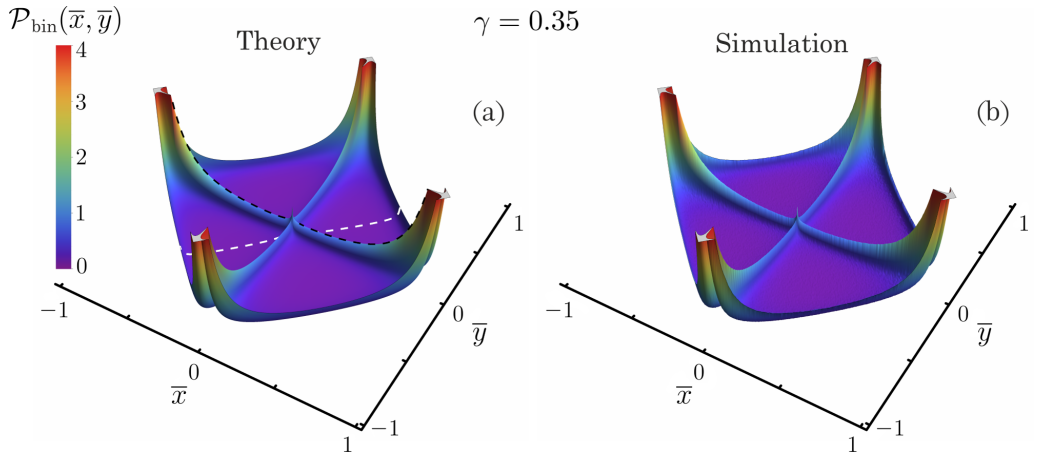

FIG. 3. Averaged probability density functions $\mathcal{P}_{\rm bin}(\overline{x},\overline{y})$ for $\gamma = 0.35$ obtained (a) with Eq. (54) and (b) by sampling a histogram for $t = 10^3$ with 10^8 realizations. To calculate the functions, the square $[-1, 1] \times [-1, 1]$ was divided into a grid of 400×400 with cells. Sections $\overline{y} = 0$ (black dashed line) and $\overline{y} = \overline{x}$ (white dashed line) are presented on Figs. 5(a) and 6(a), respectively.

using the same grid), obtained with a finite-time sampling. While for $\gamma = 0.35$ and 0.5 sampling for $t = 10^3$ yields histograms that are in a perfect agreement with the theoretical results, for $\gamma = 0.75$ the peak at the origin develops slowly in time. This is because of the proximity to the super-diffusion threshold, $\gamma = 1$, beyond which asymptotic scaling do not exist.

VI. EXACT SOLUTION FOR $\gamma = 1/2$

For $\gamma = 1/2$ we have Lévy-Smirnov distribution [18]

$$\ell_{1/2}(t) = \frac{e^{-1/(4t)}}{2\sqrt{\pi}t^{3/2}}.$$

By substituting it into Eq. (43), after some elementary calculations, we obtain

$$\mathcal{P}(\overline{x},\overline{y}) = \frac{4}{\pi^2(1-|\overline{x}|-|\overline{y}|)^3}\int_0^1 \frac{d\eta\sqrt{p(\eta)}}{\widetilde{p}^2(\eta)},$$

where

$$p(\eta) = (1+x_r-\eta)(1-\eta)\eta(\eta+y_r) \tag{55}$$

and

$$\widetilde{p}(\eta) = p(\eta)\left(\frac{1}{1+x_r-\eta}+\frac{1}{1-\eta}+\frac{1}{\eta}+\frac{1}{\eta+y_r}\right).$$

Next, we take into account that

$$\widetilde{p}(\eta) = -(2+x_r+y_r)(\eta-\eta_1)(\eta-\eta_2),$$

where

$$\eta_{1,2} = \frac{1+x_r \pm \sqrt{(1+x_r)(1+y_r)(1+x_r+y_r)}}{2+x_r+y_r}. \tag{56}$$

Since $1-|\overline{x}|-|\overline{y}| = \frac{2}{2+x_r+y_r}$ [as it follows from Eq. (42)], we can recast the expression for the asymptotic pdf in the form

$$\mathcal{P}(\overline{x},\overline{y}) = \frac{2+x_r+y_r}{2\pi^2}\int_0^1 \frac{d\eta\sqrt{p(\eta)}}{(\eta-\eta_1)^2(\eta-\eta_2)^2}. \tag{57}$$

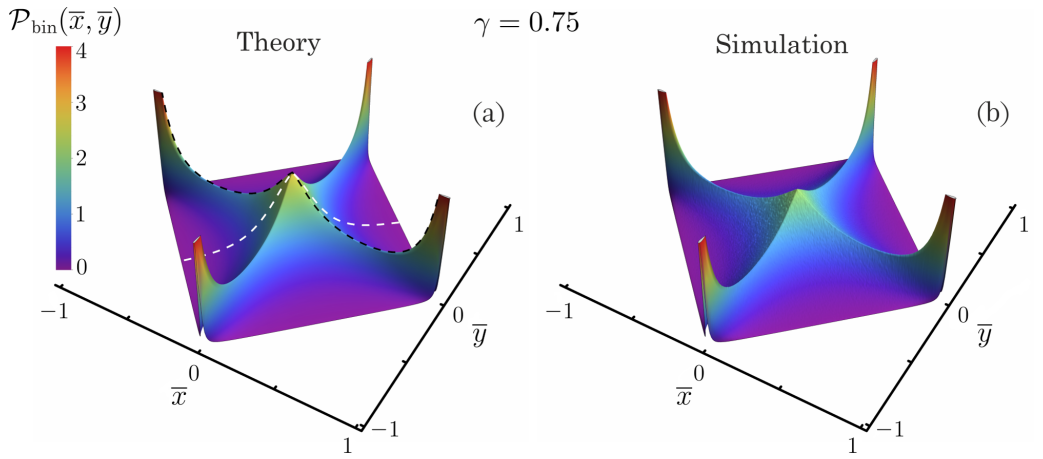

FIG. 4. Averaged probability density functions $\mathcal{P}_{\rm bin}(\overline{x},\overline{y})$ for $\gamma = 0.75$ obtained (a) with Eq. (54) and (b) by sampling a histogram for $t = 10^3$ with 10^8 realizations. To calculate the functions, the square $[-1, 1] \times [-1, 1]$ was divided into a grid of 400×400 bins. Distributions along the sections $\overline{y} = 0$ (black dashed line) and $\overline{y} = \overline{x}$ (white dashed line) are presented on Figs. 5(c) and 6(c), respectively.

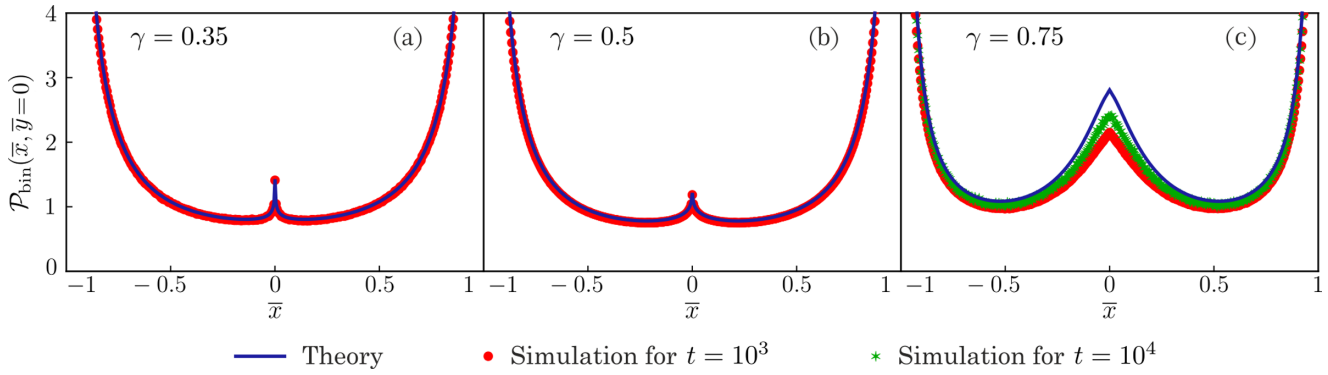

FIG. 5. Sections of $\mathcal{P}_{\rm bin}(\bar{x}, \bar{y})$ along line $\bar{y} = 0$ for three different values of γ. Blue solid curves are theoretic results, red circles are result of the sampling for time $t = 10^3$, and green stars [on panel (c)] are result of the sampling for time $t = 10^4$. Number of the sampled realisations is 10^8 in all the cases.

Because $p(\eta)$ is polynomial of the fourth order, the integral in Eq. (57) can be expressed through elliptic integrals [23] (see Appendix B for more details):

$$\mathcal{P}(\bar{x}, \bar{y}) = \Omega(\bar{x}, \bar{y})\left[\left(\mu(\bar{x}, \bar{y}) + \frac{1}{\mu(\bar{x}, \bar{y})}\right)K\left(1 - \frac{1}{\mu^2(\bar{x}, \bar{y})}\right) - 2\mu(\bar{x}, \bar{y})E\left(1 - \frac{1}{\mu^2(\bar{x}, \bar{y})}\right)\right], \tag{58}$$

where

$$\Omega(\bar{x}, \bar{y}) = \frac{(2 + x_r + y_r)^3}{16\pi^2} \times \frac{\sqrt{(1 + x_r)(1 + y_r)} - \sqrt{1 + x_r + y_r}}{(1 + x_r)(1 + y_r)(1 + x_r + y_r)}, \tag{59}$$

$$\mu(\bar{x}, \bar{y}) = \frac{\sqrt{(1 + x_r)(1 + y_r)} + \sqrt{1 + x_r + y_r}}{\sqrt{(1 + x_r)(1 + y_r)} - \sqrt{1 + x_r + y_r}}, \tag{60}$$

with $K(m)$ and $E(m)$ being complete elliptic integrals of the first and second kind, respectively.

A. Spatial asymptotic behavior of $\mathcal{P}(\bar{x}, \bar{y})$ for $\gamma = 1/2$

Here we consider the asymptotic behavior of the pdf in three different domains: (a) along one of the basis axes, (b) near the ballistic front, and (c) near one of the four ballistic peaks. In all cases we address the leading terms only.

Case (*a*). Here we consider $\mathcal{P}(\bar{x}, \bar{y})$ along the whole line $\bar{y} = 0$ except the origin and the corners of the ballistic front, i.e., $|\bar{y}| \to 0$, $|\bar{x}| \nrightarrow 0$ and $1 - |\bar{x}| \nrightarrow 0$. Due to the invariance of $\mathcal{P}(\bar{x}, \bar{y})$ with respect to the permutation $\bar{x} \leftrightarrow \bar{y}$, the results also apply to the case $\bar{x}$ ($|\bar{x}| \to 0$, $|\bar{y}| \nrightarrow 0$ and $1 - |\bar{y}| \nrightarrow 0$).

From Eqs. (42) and (60) it follows that in this domain we have $\mu(\bar{x}, \bar{y}) \to \infty$. Then, denoting $z = 1 - 1/\mu^2(\bar{x}, \bar{y})$, we see that the asymptotics of functions $K(z)$ and $E(z)$ at $z \to 1^-$ have to be found.

It is noteworthy that the complete elliptic integrals of the first and second orders can be recast by using the hypergeometric functions, namely, $K(z) = \frac{\pi}{2}{}_2F_1(\frac{1}{2}, \frac{1}{2}; 1; z)$ and $E(z) = \frac{\pi}{2}{}_2F_1(-\frac{1}{2}, \frac{1}{2}; 1; z)$. Then, by taking into account properties of hypergeometric functions [24], it is straightforward to show that for $K(z)$ and $E(z)$ the following series expansions hold:

$$K(z) \simeq -\frac{1}{2}\ln\left(\frac{1 - z}{16}\right) + O[(1 - z)\ln(1 - z)], \tag{61}$$

$$E(z) \simeq 1 + O[(1 - z)\ln(1 - z)] \tag{62}$$

at the limit $z \to 1$. In the complex z-plane functions $K(z)$ and $E(z)$ have branch cut along the real axis from $z = 1$ to ∞, therefore, the expressions are valid for real $z \to 1^-$, as required.

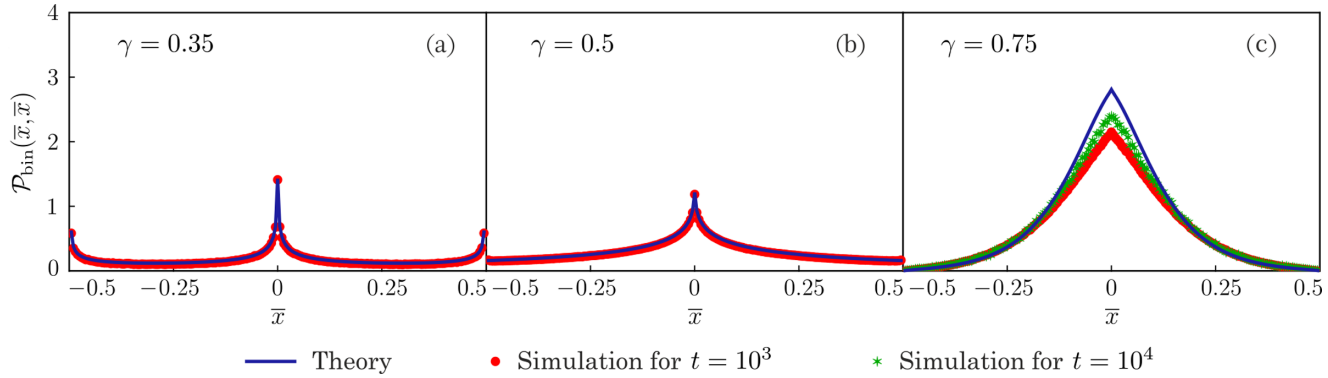

FIG. 6. Sections of $\mathcal{P}_{\rm bin}(\bar{x}, \bar{y})$ along line $\bar{y} = \bar{x}$ for three different values of γ. Blue solid curves are theoretic results, red circles are result of the sampling for time $t = 10^3$, and green stars [on panel (c)] are result of the sampling for time $t = 10^4$. Number of the sampled realisations is 10^8 in all the cases.

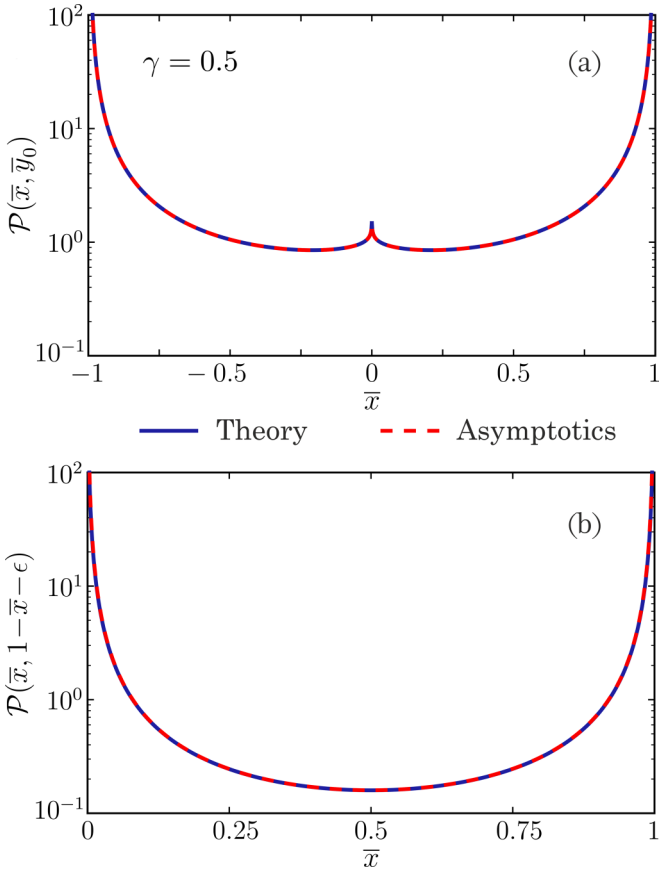

FIG. 7. Sections of re-scaled pdf $\mathcal{P}(\bar{x}, \bar{y})$ (blue solid lines), Eq. (26), for $\gamma = 1/2$ and its asymptotic expressions (red dashed lines) (a) along the line $\bar{y} = \bar{y}_0 = 10^{-3}$, Eq. (63), and (b) along the line $\bar{x} + \bar{y} = 1 - \epsilon$ with $\epsilon = 10^{-3}$, Eq. (65).

Hence, taking into account Eqs. (61) and (62), and expansions of functions $\mu(\bar{x}, \bar{y})$ and $\theta(\bar{x}, \bar{y})$ at $|\bar{y}| \to 0$ ($|\bar{x}| \nrightarrow 0$ and $1 - |\bar{x}| \nrightarrow 0$) [see Eqs. (59) and (60)], one obtains

$$\mathcal{P}(\bar{x}, \bar{y}) \simeq \frac{1}{\pi^2 (1 - \bar{x}^2)^{3/2}} \ln\left[\frac{4(1 - \bar{x}^2)}{e^2 |\bar{x}\,\bar{y}|}\right], \tag{63}$$

where we neglected all the terms of the infinitesimal order. Therefore, in case (a) the pdf has a logarithmic singularity. On Fig. 7(a) we compare sections of the rescaled pdf (obtained by using the exact expression) to the ones obtained by using the corresponding asymptotics.

Case (*b*). Here we consider the pdf at the vicinity of the ballistic front (excluding the corners), i.e., in the limit $1 - |\bar{x}| - |\bar{y}| \to 0$ with $|\bar{x}| \nrightarrow 1$ and $|\bar{y}| \nrightarrow 1$. As in the previously considered case, we will evaluate only leading term of asymptotics, but in this case with respect to $1 - |\bar{x}| - |\bar{y}|$ (instead of $|\bar{y}|$).

In the considered domain, as follows from Eqs. (42) and (60), $\mu(\bar{x}, \bar{y}) \to 1$. Then, using the Taylor series for $K(z)$ and $E(z)$ at $z \to 0$,

$$K(z) \simeq \frac{\pi}{2} + \frac{\pi z}{8} + O(z^2), \quad E(z) \simeq \frac{\pi}{2} - \frac{\pi z}{8} + O(z^2), \tag{64}$$

and the asymptotics of functions $\mu(\bar{x}, \bar{y})$ and $\theta(\bar{x}, \bar{y})$ at $1 - |\bar{x}| - |\bar{y}| \to 0$ ($|\bar{x}| \nrightarrow 1$ and $|\bar{y}| \nrightarrow 1$), we get

$$\mathcal{P}(\bar{x}, \bar{y}) \simeq \frac{1}{16\pi |\bar{x}\,\bar{y}|^{3/2}}. \tag{65}$$

Again, here we neglected all the terms of the infinitesimal order. The pdf is finite and along the lines $|\bar{x}| + |\bar{y}| = 1$ reaches minimal value $\mathcal{P}(\bar{x}, \bar{y}) = 1/(2\pi)$ in the middle points with $|\bar{x}| = |\bar{y}| = 1/2$. Sections of $\mathcal{P}(\bar{x}, \bar{y})$ and its asymptotic expressions are compared in Fig. 7(b).

Case (*c*). Here we evaluate the shape of $P_{XY}(x, y, t)$ at the corners of the ballistic front. We address the corners $|\bar{y}| \to 0$ and $|\bar{x}| \to 1$ (for other two, $|\bar{x}| \to 1$ and $|\bar{y}| \to 0$, the corresponding results can be obtained by swapping $\bar{x}$ and $\bar{y}$).

In this limit, $|\bar{y}|$ and $1 - |\bar{x}|$ are small and formally both can be used as expansion parameters. The pdf can be considered as a two-dimensional function with respect to these variables and therefore asymptotic expansions of the function will depend on the path along which the limit of small $|\bar{y}|$ and $1 - |\bar{x}|$ is approached. Here we consider two regimes, $|\bar{y}| \ll 1 - |\bar{x}|$ and $|\bar{y}| \propto 1 - |\bar{x}|$.

If we approach the corner at $|\bar{y}| \ll 1 - |\bar{x}|$ it is not difficult to demonstrate that the result derived in case (a) apply here as well. This is due to the fact that in the considered domain similar calculations can also be performed provided that $\frac{|\bar{y}|}{1-|\bar{x}|} \to 0$. Consequently, asymptotic expansion Eq. (63) holds but because of the contribution from the vicinity of $|\bar{x}| = 1$ (not only of $|\bar{y}| = 0$, as before), the singularity becomes stronger.

Finally, we approach the corner along line $|\bar{y}| \propto 1 - |\bar{x}|$, i.e., when $\mathcal{P}(\bar{x}, \bar{y})$ approaches points $(\bar{x} = \pm 1, \bar{y} = 0)$ along the lines $|\bar{x}| + c|\bar{y}| = 1$ with arbitrary $c > 1$.

Under these conditions, we have $|\bar{y}| \to 0$, $1 - |\bar{x}| \to 0$ and $1 - |\bar{x}| - |\bar{y}| = O(|\bar{y}|) = O(1 - |\bar{x}|)$. By evaluating corresponding asymptotics of $\mu(\bar{x}, \bar{y})$, $\theta(\bar{x}, \bar{y})$ and z, we find the singular leading term

$$\begin{aligned}\mathcal{P}(\bar{x}, \bar{y}) \simeq \frac{(2|\bar{x}|)^{-3/2}}{\pi^2 (1 - |\bar{x}| - |\bar{y}|)^{3/2}} \sqrt{\frac{z_r - 1}{z_r + 1}} \left(1 - \sqrt{\frac{z_r - 1}{z_r + 1}}\right) \\ \times \left[z_r K\left(\frac{2\sqrt{z_r^2 - 1}}{z_r + \sqrt{z_r^2 - 1}}\right)\right. \\ \left. - \left(z_r + \sqrt{z_r^2 - 1}\right) E\left(\frac{2\sqrt{z_r^2 - 1}}{z_r + \sqrt{z_r^2 - 1}}\right)\right],\end{aligned} \tag{66}$$

where we introduce new variable $z_r = \frac{1-|\bar{x}|}{|\bar{y}|}$ (note that it is finite and larger than 1 in the considered domain).

In the general case, the asymptotic behavior of $\mathcal{P}(\bar{x}, \bar{y})$ is specific and depends on the value of γ. Below we briefly overview the results of the corresponding analysis [22].

In case (a), for $\gamma < 1/2$ the pdf has a power-law singularity, namely, $\mathcal{P}(\bar{x}, \bar{y}) = O(|\bar{y}|^{2\gamma - 1})$ and for $\gamma > 1/2$ $\mathcal{P}(\bar{x}, \bar{y})$ is finite (i.e., the leading term of its expansion does not depend on $\bar{y}$) and has the cusp along the basis axis. In case (b), $\mathcal{P}(\bar{x}, \bar{y}) = O[(1 - |\bar{x}| - |\bar{y}|)^{2\gamma - 1}]$, therefore, for $\gamma < 1/2$ the pdf has a power-law singularity and for $\gamma > 1/2$ it is arbitrary small. Finally, in case (c), there are power-law singularities, namely, in the limit $|\bar{y}| \ll 1 - |\bar{x}|$ for $\gamma < 1/2$ the singularity

order is $O[\frac{|\bar{y}|^{2\gamma-1}}{(1-|\bar{x}|)^{1+\gamma}}]$ and for $\gamma > 1/2$ it is $O[(1-|\bar{x}|)^{\gamma-2}]$; and in the limit $|\bar{y}| \propto 1-|\bar{x}|$ the pdf has a power-law singularity of the order $O[(1-|\bar{x}|-|\bar{y}|)^{\gamma-2}]$.

VII. CONCLUSIONS

In this work we present a detailed theoretical analysis of a particular two-dimensional Lévy walk (LW) model in the ballistic regime. With this, we wanted to demonstrate that a planar spatially anisotropic LW process [4] can be evaluated analytically up to fine details. This is highlighted with Eqs. (26) and (28), which show that in this case the pdf can be represented as a sum of four single integrals. By noting that these integrals belong to the class of the so-called "integrals with weak singularities" [25,26] and using Gauss-Jacobi quadratures [20], we found a way to make an accurate comparison of these results with the numerically sampled finite-time probability distributions.

Perhaps the most prominent feature of the pdf's is the singularities and cusps (depending on γ) going along the ballistic front, $|\bar{x}|+|\bar{y}|=1$, and the principal axes. The singularities at the corners of the ballistic front are expected since they are present in one-dimensional case [13]. However, singularities *along* the front and axes are a new feature which appears due to the stepping into two dimensions. We presented a detailed analytic evaluation of these singularities for the case $\gamma = 1/2$.

For the general case $\gamma \neq 1/2$, the evaluation of the asymptotics is a more complicated task and the analysis could be performed [22] by using results obtained for the asymptotic behavior of integrals with weak singularities [25,26]. Here we would like to mention one of the main outcomes that is, near the ballistic front, pdf $\mathcal{P}(\bar{x},\bar{y})$ has the order $O[(1-|\bar{x}|-|\bar{y}|)^{2\gamma-1}]$. Therefore, the change of the front is discontinuous with γ, namely, $\mathcal{P}(\bar{x},\bar{y}) \to \infty$ for $\gamma < 1/2$, $\mathcal{P}(\bar{x},\bar{y})$ is finite for $\gamma = 1/2$, and $\mathcal{P}(\bar{x},\bar{y}) \to 0$ for $\gamma > 1/2$. It is interesting to compare our case to the case of the uniform LWs. Unfortunately, the behavior of the pdf near the ballistic front and character of a (possible) singularity are not addressed in Refs. [5,6]. We expect that the singularity is of the power-law type, with the exponent depending on the parameter γ. However, a more detailed analysis has to be performed to corroborate this statement.

Our work constitutes a next step in the direction set in Refs. [10,12], where this program was realized for the border between diffusion and super-diffusion, i.e., for $\gamma = 2$. The super-diffusive regime, $1 < \gamma < 2$, is partially addressed in Ref. [7]. This regime, however, is the hardest one to evaluate analytically. In this case $P(x,y,t)$ does not obey a universal scaling but rather two different ones, a Lévy scaling governing the bulk of the pdf and covariant scaling [27] governing the ballistic ends. In 2D, due to the dependence of the scaling functions on the direction, the position of the "meeting" point of the two functions depends now not only on time (as in the one-dimensional case [27]) but also on the direction. We hope that a progress will be made in analysis of the super-diffusive regime and it would be possible, e.g., to relate analytical results and numerical simulations of the transport in two-dimensional Hamiltonian systems [8].

ACKNOWLEDGMENTS

S.D. appreciates the hospitality of the Max Planck Institute for the Physics of Complex Systems (Dresden, Germany) where the project was finalized.

APPENDIX A: INVERSE FOURIER-LAPLACE TRANSFORM IN 1D CASE

Here we briefly review the method presented by Godrèche and Luck in Ref. [17].

Assume there is scaling $G(x,t) = \frac{1}{t}\Phi(\frac{x}{t})$. We denote $\bar{x} = \frac{x}{t}$ and obtain

$$G(k,s) = \mathcal{F}_x\mathcal{L}\{G(x,t)\} = \int_{-\infty}^{\infty} \frac{\Phi(\bar{x})d\bar{x}}{ik\bar{x}+s} = \frac{1}{s}\left\langle \frac{1}{1+\frac{ik}{s}\overline{X}} \right\rangle = \frac{1}{s} g\left(\frac{ik}{s}\right). \tag{A1}$$

According to the Sokhotski–Plemelj theorem [28]

$$\lim_{\epsilon\to 0^+} \frac{1}{\xi \pm i\epsilon} = \mp i\pi\delta(\xi) + \mathscr{P}\frac{1}{\xi}$$

(a letter $\mathscr{P}$ denotes that the Cauchy principal value is taken), and therefore, $\delta(\xi) = -\frac{1}{\pi}\mathrm{Im}\lim_{\epsilon\to 0^+}\frac{1}{\xi+i\epsilon}$.

Then, taking into account that

$$\Phi(\bar{x}) = \langle \delta(\bar{x}-\overline{X})\rangle, \tag{A2}$$

we obtain

$$\Phi(\bar{x}) = -\frac{1}{\pi}\mathrm{Im}\lim_{\epsilon\to 0^+}\left\langle \frac{1}{\bar{x}-\overline{X}+i\epsilon}\right\rangle = -\frac{1}{\pi}\lim_{\epsilon\to 0^+}\mathrm{Im}\left[\frac{1}{\bar{x}+i\epsilon} g\left(-\frac{1}{\bar{x}+i\epsilon}\right)\right]. \tag{A3}$$

Therefore,

$$G(x,t) = -\frac{1}{\pi x}\lim_{\epsilon\to 0^+}\mathrm{Im}\, g\left(-\frac{1}{x/t+i\epsilon}\right). \tag{A4}$$

Next we show that the method proposed by Godrèche and Luck is related to the Stieltjes transform.

Namely, from Eq. (A1) follows (here we introduce notation $ik/s = \zeta$)

$$g(\zeta) = \int_{-\infty}^{\infty} \frac{\Phi(\bar{x})d\bar{x}}{1+\zeta\,\bar{x}}.$$

We replace $\zeta = -1/z$ and obtain

$$\frac{1}{z}g\left(-\frac{1}{z}\right) = \int_{-\infty}^{\infty}\frac{\Phi(\bar{x})d\bar{x}}{z-\bar{x}}. \tag{A5}$$

The right-hand side of Eq. (A5) is the Stieltjes transform of $\Phi(\bar{x})$. Denoting $\mathcal{S}(z) = \frac{1}{z}g(-\frac{1}{z})$, taking into account that the inverse Stieltjes transform is defined as [29]

$$\Phi(\bar{x}) = \lim_{\epsilon\to 0^+}\frac{\mathcal{S}(\bar{x}-i\epsilon)-\mathcal{S}(\bar{x}+i\epsilon)}{2\pi i},$$

and using the identity $\mathrm{Im}\, f = \frac{f-f^*}{2i}$, we arrive at the Eq. (A3).

Therefore, it is clear now that the method, in principle, is a particular case of the implementation of the inverse Stieltjes

transform. Usually it is used for the probability density functions. However, it is not specific and can be used for general functions [29], like functions in Eqs. (13) and (14).

APPENDIX B: LEGENDRE'S NORMAL FORM FOR ELLIPTIC INTEGRALS

Assume that $R(\eta)$ is a fourth-order polynomial and $S(\eta)$ is an arbitrary rational function. We will follow Ref. [23] (Sec. VIII in there), and describe a method to reduce integrals of the following type:

$$I = \int_0^1 \frac{S(\eta)d\eta}{\sqrt{R(\eta)}} \tag{B1}$$

to elliptic ones. We are only interested in the case when all roots of $R(\eta)$ are real; we also set the leading coefficient of the polynomial equals to one. We write $R(\eta) = (\eta - a_1)(\eta - a_2)(\eta - a_3)(\eta - a_4)$ and apply to Eq. (B1) the following linear fractional transform

$$\eta = \frac{a\omega + b}{c\omega + d}, \tag{B2}$$

where we also assume $ad - bc \neq 0$. Next we take into account that

$$\eta - a_j = \frac{(a - ca_j)\omega + b - da_j}{c\omega + d},$$

with $j = \overline{1,4}$ and

$$d\eta = \frac{ad - bc}{(c\omega + d)^2} d\omega,$$

and arrive at

$$I = \int_{-\frac{b}{a}}^{-\frac{b-d}{a-c}} \frac{(ad - bc)\sigma(\omega)d\omega}{\sqrt{\prod_{j=1}^{4}[(a - ca_j)\omega + b - da_j]}}, \tag{B3}$$

where $\sigma(\omega) = S(\frac{a\omega+b}{c\omega+d})$ is a rational function.

Next we write

$$\prod_{j=1}^{4}[(a - ca_j)\omega + b - da_j] = (q_0\omega^2 + q_1\omega + q_2) \times (h_0\omega^2 + h_1\omega + h_2), \tag{B4}$$

with coefficients

$$\begin{aligned}
q_0 &= (a - ca_1)(a - ca_2),\\
q_1 &= (a - ca_1)(b - da_2) + (a - ca_2)(b - da_1),\\
q_2 &= (b - da_1)(b - da_2),\\
h_0 &= (a - ca_3)(a - ca_4),\\
h_1 &= (a - ca_3)(b - da_4) + (a - ca_4)(b - da_3),\\
h_2 &= (b - da_3)(b - da_4).
\end{aligned}$$

We choose a, b, c, d such that in polynomial Eq. (B4) coefficients for ω^3 and ω are nullified. Whence it follows conditions

$$q_0h_1 + h_0q_1 = 0, \quad q_1h_2 + h_1q_2 = 0,$$

which hold for $q_1 = h_1 = 0$.

We obtain therefore a system of equations:

$$\begin{aligned}
2 - \left(\frac{d}{b} + \frac{c}{a}\right)(a_1 + a_2) + 2\frac{d}{b}\frac{c}{a}a_1a_2 = 0,\\
2 - \left(\frac{d}{b} + \frac{c}{a}\right)(a_3 + a_4) + 2\frac{d}{b}\frac{c}{a}a_3a_4 = 0,
\end{aligned} \tag{B5}$$

from which the expressions for $\frac{d}{b} + \frac{c}{a}$ and $\frac{d}{b}\frac{c}{a}$ can be obtained. From four variables a, b, c, d we can choose two as parameters and solve the system of equations for the remaining two. Integral in Eq. (B3) can be written now as

$$I = \int_{-\frac{b}{a}}^{-\frac{b-d}{a-c}} \frac{(ad - bc)\sigma(\omega)d\omega}{\sqrt{(q_0\omega^2 + q_2)(h_0\omega^2 + h_2)}}, \tag{B6}$$

and can be reduced to a combination of elliptic integrals of the first, second, and third orders [23].

We apply the above described approach to the integral in Eq. (57)

$$I = \int_0^1 \frac{d\eta}{\sqrt{p(\eta)}} \frac{p(\eta)}{(\eta - \eta_1)^2(\eta - \eta_2)^2}. \tag{B7}$$

We set $R(\eta) = p(\eta)$, $S(\eta) = \frac{p(\eta)}{(\eta-\eta_1)^2(\eta-\eta_2)^2}$ and

$$a_1 = 1 + x_r, \quad a_2 = 1, \quad a_3 = 0, \quad a_4 = -y_r.$$

After applying the linear fractional transform Eq. (B2) with parameters $a = -1$ and $b = 1$ (just a convenient choice), we get solutions of the system Eq. (B5):

$$\begin{aligned}
c &= \frac{1 + x_r + \sqrt{D}}{(1 + x_r)y_r}, \quad d = -\frac{1 + x_r - \sqrt{D}}{(1 + x_r)y_r},\\
c &= \frac{1 + x_r - \sqrt{D}}{(1 + x_r)y_r}, \quad d = -\frac{1 + x_r + \sqrt{D}}{(1 + x_r)y_r},
\end{aligned} \tag{B8}$$

where

$$D = (1 + x_r)(1 + y_r)(1 + x_r + y_r). \tag{B9}$$

It is not important which pair to choose; we take the second one from Eq. (B8), which guarantees $ad - bc > 0$.

Thus, we get

$$\begin{aligned}
ad - bc &= \frac{2\sqrt{D}}{(1 + x_r)y_r}, \quad -\frac{b}{a} = 1,\\
-\frac{b - d}{a - c} &= \frac{(1 + x_r)(1 + y_r) + \sqrt{D}}{(1 + x_r)(1 + y_r) - \sqrt{D}},
\end{aligned}$$

and

$$\begin{aligned}
q_{0,2} &= \frac{(1 + x_r + y_r \mp \sqrt{D})[(1 + x_r)(1 + y_r) \mp \sqrt{D}]}{(1 + x_r)y_r^2},\\
h_{0,2} &= \pm\frac{\sqrt{D}}{1 + x_r}.
\end{aligned} \tag{B10}$$

After substituting Eq. (B2) and taking into account the above results, we arrive at

$$\begin{aligned}
p(\eta) &= \frac{(q_0\omega^2 + q_2)(h_0\omega^2 + h_2)}{(c\omega + d)^4},\\
q_0\omega^2 + q_2 &= |q_0|\left(\frac{q_2}{|q_0|} - \omega^2\right),\\
h_0\omega^2 + h_2 &= h_0(\omega^2 - 1),
\end{aligned}$$

$$\eta - \eta_1 = \frac{2}{c\omega + d}\frac{(1+y_r)(1+x_r+y_r)+\sqrt{D}}{(2+x_r+y_r)y_r},$$

$$\eta - \eta_2 = -\frac{2}{c\omega + d}\frac{(1+y_r)(1+x_r+y_r)-\sqrt{D}}{(2+x_r+y_r)y_r}\omega,$$

$$\sigma(\omega) = \frac{(2+x_r+y_r)^2 y_r^2}{16(1+y_r)^2(1+x_r+y_r)^2}|q_0|h_0 \times \left(-\omega^2 + \frac{q_2}{|q_0|} + 1 - \frac{q_2}{|q_0|\omega^2}\right).$$

Here we took into account that $q_0 < 0$, $h_2 < 0$ and $h_2 = -h_0$. Reducing Eq. (B6), we get

$$I = \theta \int_1^\mu \frac{d\omega}{\sqrt{\left(\frac{q_2}{|q_0|} - \omega^2\right)(\omega^2 - 1)}} \times \left(-\omega^2 + \frac{q_2}{|q_0|} + 1 - \frac{q_2}{|q_0|\omega^2}\right), \quad \text{(B11)}$$

where

$$\theta = \frac{(2+x_r+y_r)^2}{8D} \times [\sqrt{(1+x_r)(1+y_r)} - \sqrt{1+x_r+y_r}], \quad \text{(B12)}$$

$$\mu = -\frac{b-d}{a-c} = \frac{(1+x_r)(1+y_r)+\sqrt{D}}{(1+x_r)(1+y_r)-\sqrt{D}}. \quad \text{(B13)}$$

From Eq. (B10) we obtain

$$\frac{q_2}{|q_0|} = \frac{[\sqrt{D}+1+x_r+y_r][(1+x_r)(1+y_r)+\sqrt{D}]}{[\sqrt{D}-(1+x_r+y_r)][(1+x_r)(1+y_r)-\sqrt{D}]}.$$

Next we use Eq. (B9) and identity

$$\frac{\lambda_1 + \sqrt{\lambda_1\lambda_2}}{\lambda_1 - \sqrt{\lambda_1\lambda_2}} = \frac{\sqrt{\lambda_1\lambda_2} + \lambda_2}{\sqrt{\lambda_1\lambda_2} - \lambda_2},$$

and we find out

$$\frac{(1+x_r)(1+y_r)+\sqrt{D}}{(1+x_r)(1+y_r)-\sqrt{D}} = \frac{\sqrt{D}+1+x_r+y_r}{\sqrt{D}-(1+x_r+y_r)}.$$

Therefore, the following holds:

$$\mu = \frac{\sqrt{D}+1+x_r+y_r}{\sqrt{D}-(1+x_r+y_r)}, \quad \frac{q_2}{|q_0|} = \mu^2. \quad \text{(B14)}$$

Integral Eq. (B11) takes a form

$$I = \theta \int_1^\mu \frac{d\omega}{\sqrt{(\mu^2-\omega^2)(\omega^2-1)}}\left(-\omega^2 + \mu^2 + 1 - \frac{\mu^2}{\omega^2}\right).$$

It is easy to see that $-\omega^2 + \mu^2 + 1 - \frac{\mu^2}{\omega^2} \geqslant 0$ for $\omega \in [1, \mu]$, and therefore $I > 0$.

Finally, by using table integrals [30], we get

$$I = \theta[(\mu + 1/\mu)K(1 - 1/\mu^2) - 2\mu E(1 - 1/\mu^2)], \quad \text{(B15)}$$

where

$$K(m) = \int_0^{\pi/2} \frac{d\varphi}{\sqrt{1 - m\sin^2\varphi}}, \quad \text{(B16)}$$

$$E(m) = \int_0^{\pi/2} d\varphi\sqrt{1 - m\sin^2\varphi} \quad \text{(B17)}$$

are complete elliptic integrals of the first and second orders, respectively.

[1] M. F. Shlesinger, J. Klafter, and Y. Wong, Random walks with infinite spatial and temporal moments, J. Stat. Phys. **27**, 499 (1982).

[2] M. F. Shlesinger, B. J. West, and J. Klafter, Lévy Dynamics of Enhanced Diffusion: Applications to Turbulence, Phys. Rev. Lett. **58**, 1100 (1987).

[3] V. Zaburdaev, S. Denisov, and J. Klafter, Lévy walks, Rev. Mod. Phys. **87**, 483 (2015).

[4] V. Zaburdaev, I. Fouxon, S. Denisov, and E. Barkai, Superdiffusive Dispersals Impart the Geometry of Underlying Random Walks, Phys. Rev. Lett. **117**, 270601 (2016).

[5] M. Magdziarz and T. Zorawik, Explicit densities of multidimensional ballistic Lévy walks, Phys. Rev. E **94**, 022130 (2016).

[6] M. Magdziarz and T. Zorawik, Method of calculating densities for isotropic ballistic Lévy walks, Commun. Nonlin. Sci. Numer. Simul. **48**, 462 (2017).

[7] I. Fouxon, S. Denisov, V. Zaburdaev, and E. Barkai, Limit theorems for Lévy walks in d dimensions: Rare and bulk fluctuations, J. Phys. A: Math. Theor. **50**, 154002 (2017).

[8] J. Klafter and G. Zumofen, Lévy statistics in a Hamiltonian system, Phys. Rev. E **49**, 4873 (1994).

[9] L. van der Heijdt, *Face to Face with Dice: 5000 Years of Dice and Dicing* (Gopher Publishers, Groningen, 2002).

[10] L. Zarfaty, A. Peletskyi, I. Fouxon, S. Denisov, and E. Barkai, Dispersion of particles in an infinite-horizon Lorentz gas, Phys. Rev. E **98**, 010101(R) (2018).

[11] G. Cristadoro, T. Gilbert, M. Lenci, and D. P. Sanders, Measuring logarithmic corrections to normal diffusion in infinite-horizon billiards, Phys. Rev. E **90**, 022106 (2014).

[12] L. Zarfaty, A. Peletskyi, E. Barkai, and S. Denisov, Infinite horizon billiards: Transport at the border between Gauss and Lévy universality classes, Phys. Rev. E **100**, 042140 (2019).

[13] D. Froemberg, M. Schmiedeberg, E. Barkai, and V. Zaburdaev, Asymptotic densities of ballistic Lévy walks, Phys. Rev. E **91**, 022131 (2015).

[14] M. M. Meerschaert, D. A. Benson, H.-P. Scheffler, and P. Becker-Kern, Governing equations and solutions of anomalous random walk limits, Phys. Rev. E **66**, 060102(R) (2002).

[15] I. M. Sokolov and R. Metzler, Towards deterministic equations for Lévy walks: The fractional material derivative, Phys. Rev. E **67**, 010101(R) (2003).

[16] R. Metzler and J. Klafter, The restaurant at the end of the random walk: Recent developments in the description of anomalous transport by fractional dynamics, J. Phys. A: Math. Gen. **37**, R161 (2004).

[17] C. Godrèche and J. M. Luck, Statistics of the occupation time of renewal processes, J. Stat. Phys. **104**, 489 (2001).

[18] G. Samorodnitsky and M. S. Taqqu, *Random Processes: Stochastic Models with Infinite Variance Stable Non-Gaussian* (Chapman and Hall, New York, 1994).

[19] Formally, $x_r = x_t$ and $y_r = y_t$. However, since variables x_r and y_r are related to the expression which does not depend on t explicitly, we use different notations here to distinguish these two different situations.

[20] P. J. Davis and P. Rabinowitz, *Methods of Numerical Integration* (Academic Press, Orlando, FL, 1984).

[21] An alternative is to split expression in Eq. (45) into summands of two different types, which do and do not include singular multiplier $(1-\eta)^{\gamma-1}$. However, in this case we would need two different types of orthogonal polynomials; e.g., for weights w_j and nodes η_j.

[22] Yu. S. Bystrik and S. Denisov (unpublished).

[23] H. Hancock, *Lectures on the Theory of Elliptic Functions* (John Wiley & Sons, New York, NY, 1910), Vol. I.

[24] H. Bateman and A. Erdélyi, *Higher Transcendental Functions* (McGraw-Hill, New York, 1953), Volume 1.

[25] M. V. Fedoryuk, *Asymptotics: Integrals and Series* (Nauka, Moscow, 1987) [in Russian].

[26] M. V. Fedoryuk, *Asymptotic Methods in Analysis*, in: Gamkrelidze, R. V. (Ed.), *Analysis I. Integral Representations and Asymptotic Methods* (Springer, Berlin, 1989).

[27] A. Rebenshtok, S. Denisov, P. Hänggi, and E. Barkai, Non-Normalizable Densities in Strong Anomalous Diffusion: Beyond the Central Limit Theorem, Phys. Rev. Lett. **112**, 110601 (2014).

[28] V. S. Vladimirov, *Equations of Mathematical Physics* (Dekker, New York, 1971).

[29] D. V. Widder, *The Laplace Transform* (Princeton University Press, Princeton, NJ, 1946).

[30] A. P. Prudnikov, Yu. A. Brychkov, and O. I. Marichev, *Integrals and Series: Elementary Functions* (Taylor & Francis, London, 2002), Volume 1.